

# Tackling On-Shell Diagrams without External BCFW-Bridges by Auxiliary Momentum Legs

---

**Baoyi Chen, Gang Chen, Yeuk-Kwan E. Cheung, Ruofei Xie, and Yuan Xin**

*Department of Physics, Nanjing University, 22 Hankou Road, Nanjing 210098, China*

*E-mail:* [gang.chern@gmail.com](mailto:gang.chern@gmail.com), [cheung@nju.edu.cn](mailto:cheung@nju.edu.cn)

## ABSTRACT:

On-shell diagrams [1] have become an important tool employed in the study of  $\mathcal{N} = 4$  scattering amplitudes since its introduction by Arkani-Hamed et al in a seminal work [2]. In this work we extend these techniques to higher-loop nonplanar on-shell diagrams without external BCFW-bridges. To compute the leading singularities for these diagrams we introduce an auxiliary external momentum line so that we can, again, deploy the systematic method introduced in [18] to decompose the on-shell diagrams by successive BCFW-bridges and reduce it to planar diagrams—using the CCD permutation relation of Yangian invariants [17]—whose top-forms are well-known. The top-form of the on-shell diagram with the auxiliary line can then be obtained by performing the chain of BCFW-integrations in the inverse order, as prescribed in our companion paper. To recover the top-form of the original diagram without the external BCFW-bridge, a soft limit for the auxiliary line is taken. We obtain the evolutions of the Grassmannian integral and the geometric constraints under the soft limit. This, together with [18], completes the top-form description of leading singularities in nonplanar scattering amplitudes of  $\mathcal{N} = 4$  Super Yang-Mills (SYM) which is valid for arbitrary higher-loops beyond MHV (Maximally-Helicity-Violation).

**KEYWORDS:** Nonplanar Amplitudes, Non-positive Grassmannians,  $N=4$  Supersymmetric Yang-Mills, Unitarity Cuts, BCFW

ARXIV EPRINT: [1507.03214](https://arxiv.org/abs/1507.03214)

---

## Contents

1	Introduction	1
2	BCFW-reduction of the leading singularities	2
3	Construction of the top-form	3
4	Construction the top-form of no-bridge diagrams	6
5	Rational top-forms and rational soft limit:	7
6	More Examples	9
7	Summary and Outlook	17
8	Acknowledgments	18

---

## 1 Introduction

Bipartite, or on-shell diagrams, and the associated Grassmannian geometry [1], have recently found their way in the scattering amplitude computations; in particular, scattering amplitudes in the  $\mathcal{N} = 4$  Supersymmetric Yang-Mills (SYM) are conveniently casted into this new language [2] to be rid of gauge redundancy. Since then breathtaking progress has been made in the computations of the planar scattering amplitudes in  $\mathcal{N} = 4$  SYM theory [3–10]. Planar scattering amplitudes are represented by on-shell bipartite diagrams and expressed in the “top-form” in contour integrations over the Grassmannian submanifolds. Planar loop integrands in  $\mathcal{N} = 4$  SYM have recently been constructed in [3, 11]. In this seminal work [3], the Grassmannian and on-shell method [1] was introduced to the physicists. As a result, the “ $d\log$ ” form and the Yangian symmetry [12–16] of the scattering amplitudes are made manifest in the planar limit.

It is natural to extend the construction to non-planar scattering amplitudes [17–27], and theories with reduced (super) symmetries [28–30]. In [17] general unitarity cuts method are applied to nonplanar on-shell diagrams to address the ordering ambiguity of the external momenta due to non-planarity. A permutation relation (CCD-relation)

of Yangian invariants was discovered in on-shell diagrams, which allows an exchange of two external momenta. Thus it relates a nonplanar on-shell diagram to a planar one. (See also [31].) A systematic chain of BCFW-bridge reductions was then used to compute the nonplanar diagram and proved that the nonplanar diagram is related to a linear combination of the planar ones with kinematic coefficients [17]—paving the way for further investigations of nonplanar amplitudes [2, 17, 18, 20, 21, 31–34] and the possibility of extended hidden symmetries existing in the nonplanar amplitudes [35–37].

Whereas the leading singularities are represented in the *top-form* in the Grassmannian integrals in which the integrands are comprised of rational functions of minors of the constraint matrices  $\{\mathbf{R}(M_C)\}$ , the amplitude structures are simple and compact when expressed in the top-form. And the Yangian symmetry is manifest in the positive diffeomorphisms of positive Grassmannian geometry [3]. It is therefore crucial to express scattering amplitudes in the top-form in order to exploit its power to further uncover hidden symmetries and dualities of the scattering amplitudes. We present in this note a construction of the top-forms for nonplanar scattering amplitudes, building on our earlier work of unveiling the first class of nonplanar Yangian permutation relations [17]. Our method applies to all leading singularities beyond MHV and at arbitrary higher-loops.

## 2 BCFW-reduction of the leading singularities

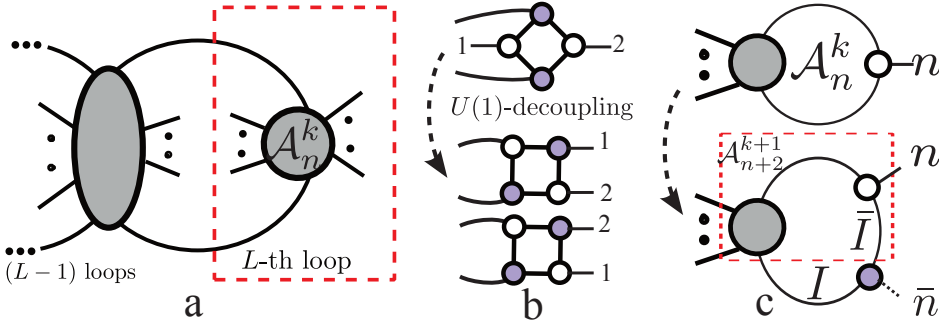


**Figure 1.** (a) Obtaining the  $L$ -th loop amplitude recursively. (b) Utilizing the CCD permutation relation to turn a nonplanar diagram into a planar one. (c) Introduction of an auxiliary external momentum line to form a BCFW bridge.

In [18, 19] we introduced a systematic way of decompose a given  $L$ -loop nonplanar diagram by BCFW-bridges, reductively, to three equivalence classes of trivial graphs. Nonplanar subgraphs were converted to a linear combination of planar ones with kinematic coefficients by CCD permutation [17] as shown in Fig. 1 (b). Attaching the BCFW-bridges in the reverse order one can straightforwardly obtain an analytic expression of the leading singularities.

For sub-diagrams that are BCFW-decomposable, we perform according to the recipe presented in [18, 19]. There exist, however, “no-bridge” diagrams which do not contain any external BCFW bridges [18, 21].

In this work we present a general method applicable to any on-shell diagrams without external BCFW-bridges. The trick is to add an auxiliary external momentum line to form an *auxiliary BCFW bridge*, shown in Fig. 1 (c). To regain the original no-bridge diagram we take the soft limit [38–40], to set the auxiliary momentum to zero. In this way the chain of BCFW reductions for the nonplanar on-shell diagrams can be obtained.

In the rest of the letter we present a recipe for the construction of the *top-form*, by BCFW reductions [18], upon adding an auxiliary external momentum line.

### 3 Construction of the top-form

The top-form of an on-shell diagram is obtained once the geometric constraints,  $\Gamma$ , and the integrand,  $f(C)$ , are determined. A non-planar leading singularity in the form [3]

$$\mathcal{T} = \oint_{\Gamma} \frac{dC^{k \times n}}{\text{Vol}(GL(k))} \frac{\delta^{k \times 4}(C \cdot \tilde{\eta})}{f(C)} \delta^{k \times 2}(C \cdot \tilde{\lambda}) \delta^{2 \times (n-k)}(\lambda \cdot C^{\perp}) .$$

requires the calculation of  $f(C)$  and  $\Gamma$  under the BCFW shifts, and then taking soft limit for the auxiliary BCFW bridges.

Let us study the BCFW shifts. The integrand,  $f(C)$ , must contain those poles equivalent to the constraints in  $\Gamma$ ; otherwise the contour integration around  $\Gamma$  vanishes. Each BCFW bridge removes one pole in  $f(C)$  by shifting a zero minor to be nonzero: in nontrivial cases the poles in the integrand must change their forms and the integrand changes its functional form accordingly. To see this, we parametrize the constraint matrix,  $C$ , using the BCFW parameter,  $\alpha$ . In a BCFW shift, a column vector  $X$  is shifted:  $X \rightarrow \hat{X} = X + \alpha Y$ , with several minors of  $f(C)$  become functions of  $\alpha$ . After the shift, there exists at least one constraint  $M_0(X) = 0$  being shifted to  $M_0(\hat{X}) = M_0(X) + \alpha R(Y)$  if there is a top-form. This will be demonstrated in the following section. Meanwhile the factor  $M_0(\hat{X})$  should be presented in the denominator to contribute a pole at  $\alpha = 0$ . In other words  $\alpha = M_0(\hat{X})/R(Y)$  is then a rational function of  $\hat{C}$  and therefore can be subtracted from other shifted minors to obtain certain shift-invariant minors of  $\hat{C}$ ,  $M_i(X) = M_i(\hat{X} - \alpha Y)$ . In summary upon attaching a BCFW bridge the integrand becomes

$$f(\hat{C}) = M_0(\hat{X}) \prod_i M_i(\hat{X} - \alpha Y) \times \left( \begin{array}{c} \text{minors} \\ \text{without } \alpha \end{array} \right) . \quad (3.1)$$

We shall present our techniques in several examples below:

1. a six-point three-loop MHV nonplanar amplitude with one auxiliary line,
2. an  $\overline{MHV}$  example with one auxiliary line,
3. a non-planar NMHV 4-loop example with one auxiliary line,
4. an  $N^4\text{MHV}$  example with two auxiliary lines.

The six-point three-loop MHV example has been analyzed in [21]. We include here for comparison.

### An MHV example

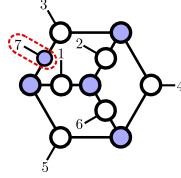


**Figure 2.** An MHV example

We attach one auxiliary external momentum line, in Fig. 2, and form an auxiliary BCFW-bridge (3, 7). This on-shell diagram can be decomposed to identity as follows,  $(1, 7) \rightarrow (2, 6) \rightarrow (3, 5) \rightarrow (2, 3) \rightarrow (3, 4) \rightarrow (12) \rightarrow (2, 3) \rightarrow (5, 7) \rightarrow (3, 7)$ . Before adding Bridge-(5, 7), the on-shell diagram is still planar. The Grassmannian constraints and the top-form can be obtained directly from the permutation [3] shown in the first row of Tab. 1. Adding Bridge-(5, 7), the constraint  $(71)^1 \rightarrow (157)^2$ , as shown in the second row of Tab. 1. Adding Bridge-(3, 7), the constraint  $(157)^2$  disappears. Before

**Table 1.** The evolution of the geometric constraints.

	$(71)^1$	$(234)^2$	$(456)^2$	$(612)^2$
(5, 7)	$(157)^2$	$(234)^2$	$(456)^2$	$(126)^2$
(3, 7)		$(234)^2$	$(456)^2$	$(126)^2$

attaching Bridge-(5, 7), the top-form is

$$\frac{1}{(123)(234)(345)(456)(567)(671)(712)}$$

When attaching (5, 7), the contour integral around the pole  $(712) = (\widehat{712}) - \alpha(512)$  is replaced by  $\frac{d\alpha}{\alpha}$  with  $\alpha = \frac{(\widehat{712})}{(512)}$ . All the minors except (712) with column 7 may be affected by the bridge

$$\begin{aligned}(567) &\rightarrow \frac{(56(\widehat{75}) \cap (12))}{(512)} = (56\widehat{7}) \\ (671) &\rightarrow \frac{(6(\widehat{75}) \cap (12)1)}{(512)} = \frac{(\widehat{715})(126)}{(512)}.\end{aligned}$$

Then the top-form integrand becomes

$$\frac{(125)}{(123)(234)(345)(456)(567)(157)(126)(127)}.$$

Similarly after attaching Bridge-(3, 7) the top-form integrand becomes

$$\frac{(135)^2}{(123)(234)(345)(456)(156)(357)(157)(126)(137)}.$$

To obtain the top-form of the original diagram we parametrize the  $C'$  as

$$\left( \begin{array}{c|c} C & 0 \\ \hline 0 & 0 \\ 0 & 0 \\ c_3 & c_4 \\ c_5 & c_6 \\ c_6 & 1 \end{array} \right).$$

We then expand all the minors in  $C'$  as those of  $C$

$$\begin{aligned}(126) &= (12)c_6 & (234) &= -c_3(24) + c_4(23) \\ (123) &= (12)c_3 & (456) &= c_4(56) - c_5(46) \\ (156) &= -(16)c_5 & (135) &= -c_3(15) + c_5(13) \\ (137) &= (13) & (345) &= c_3(45) - c_4(35) + c_5(34) \\ (357) &= (35) & (157) &= (15) .\end{aligned}$$

The top-form thus becomes

$$\begin{aligned}&\frac{(-c_3(15) + c_5(13))^2}{-(12)(35)(15)(12)(13)(16)c_3c_6c_5(-c_3(24) + c_4(23))} \\ &\times \frac{1}{(c_3(45) - c_4(35) + c_5(34))(c_4(56) - c_5(46))}.\end{aligned}$$

The additional pole is characterised by (126), (234), (456). A contour integration yields  $c_6 \rightarrow 0$ ,  $c_3 \rightarrow \frac{(23)}{(24)}c_4$ ,  $c_5 \rightarrow \frac{(56)}{(46)}c_4$  and

$$\frac{[(56)(13)(24) - (23)(15)(46)]^2}{(23)(12)(24)(26)(45)(34)(16)(56)(35)(15)(13)(46)},$$

agreeing with [21]. This can be further simplified,

$$\begin{aligned}&-f_p(125364) + f_p(125463) - f_p(134265) \\ &+ f_p(126543) - f_p(132465) - f_p(123564),\end{aligned}$$

with  $f_p$  denoting the planar amplitudes of the corresponding orders.

## 4 Construction the top-form of no-bridge diagrams

We turn our attention to the structures, other than the BCFW-shifts, arisen in the class of diagrams without external BCFW-bridges [18, 21], *no-bridge* diagrams, in short. In [18] top-forms are obtained by imposing  $U(1)$ -decoupling relation. The top forms of no-bridge diagrams after adding the auxiliary BCFW bridges can likewise be obtained using the recipe prescribed in [18]. In this section we discuss how one can recover the top-forms of the original no-bridge diagrams by taking the soft limit on the auxiliary external momentum.

The on-shell diagram  $\mathcal{A}_{n+1}^{k+1}$  with one auxiliary line, shown in Fig.1(c), can be written in two equivalent forms:

$$(I) = \int \frac{d^2\lambda_I d^2\tilde{\lambda}_I d^4\tilde{\eta}_I}{\text{vol}(GL(1))} \frac{\mathcal{A}_{n+2}^{k+1} \langle I\bar{I} \rangle^3}{\langle \bar{n}I \rangle^2 \langle \bar{I}\bar{n} \rangle} \delta([\bar{n}I]) \delta^4(\tilde{\eta}_{\bar{n}} + \frac{\langle \bar{I}\bar{n} \rangle}{\langle \bar{I}I \rangle} \tilde{\eta}_I), \quad (4.1)$$

$$(II) = \oint_{\bar{\Gamma}} \frac{dC^{k \times n} dc_{k+1} \cdots dc_n (1 \cdots k)}{\text{Vol}(GL(k)) f(C, c_i)} \\ \times \delta^{k \times 4}(C \cdot \tilde{\eta}) \delta^{k \times 2}(C \cdot \tilde{\lambda}) \delta^{2(n-k)}(\lambda \cdot C'^{\perp}) \\ \times \delta^2\left(\sum_{i=k+1}^{n, \bar{n}} c_i \tilde{\lambda}_i\right) \delta^4\left(\sum_{i=k+1}^{n, \bar{n}} c_i \tilde{\eta}_i\right), \quad (4.2)$$

where  $c_{\bar{n}} = 1$ . Eq.(4.1) is obtained from Fig.1(c) by integrating over the internal line  $\bar{I}$ . Eq.(4.2) is a general top-form of  $\mathcal{A}_{n+1}^{k+1}$ , where we choose a particular parameterization of the Grassmannian matrix  $C'$  as

$$C' = \left( \begin{array}{ccc|ccc} & & & & & & 0 \\ & & & & & & \vdots \\ & & & & & & 0 \\ \hline & & & C & & & 0 \\ 0 & \cdots & 0 & c_{k+1} & \cdots & c_n & 1 \end{array} \right).$$

Our method of adding the auxiliary line can be justified by comparing (4.1) and (4.2) and noting that

$$\delta^2\left(\sum_{i=k+1}^{n, \bar{n}} c_i \tilde{\lambda}_i\right) = \delta\left(\sum_{i=k+1}^n c_i \frac{[i1]}{[\bar{n}1]} + 1\right) \delta([\bar{n}I]),$$

(4.1) and (4.2) can be proved to both contain the term

$$\delta([\bar{n}I]) \delta^4(\tilde{\eta}_{\bar{n}} + \frac{\langle \bar{I}\bar{n} \rangle}{\langle \bar{I}I \rangle} \tilde{\eta}_I)$$

which can be removed from the overall delta function of constraints. The remaining part of (4.1) then corresponds to the no-bridge diagram  $\mathcal{A}_n^k$  in the limit of  $\lambda_{\tilde{n}} \rightarrow 0$ . On the other hand, after taking the soft limit (4.2) yields

$$\begin{aligned} \mathcal{A}_n^k = & \oint_{\Gamma} \frac{dC^{k \times n} dc_{k+1} \cdots dc_n}{\text{Vol}(GL(k))} \frac{(1 \cdots k) \delta^{k \times 4}(C \cdot \tilde{\eta})}{f(C, c_i)} \\ & \times \delta^{k \times 2}(C \cdot \tilde{\lambda}) \delta^{2 \times (n-k)}(\lambda \cdot C^\perp) \delta\left(\sum_{i=k+1}^n c_i \frac{[i1]}{[\tilde{n}1]} + 1\right). \end{aligned} \quad (4.3)$$

This is easily proven by counting the degrees of freedom of the associated on-shell diagram in which only one element  $c_f$  among  $c_i$  is a free parameter. As we shall prove in the following section, no-bridge diagrams having top-forms requires that  $c_i/c_r = \mathbf{R}(M_C)$ . Using this relation the integration  $\int \frac{dc_r}{c_r} \delta(\sum_{i=k+1}^n c_i \frac{[i1]}{[\tilde{n}1]} + 1)$  gives 1. Finally we obtain the top-form of  $\mathcal{A}_n^k$  by expanding the minors of  $C'$  into  $C$  minors in the integrand.

## 5 Rational top-forms and rational soft limit:

It is worth to remark on which kind of nonplanar on-shell diagrams can have rational top-forms. We address this question by building an equivalent relation between *rational top-form*, and *rational soft limit*: If the soft limit of auxiliary line leads to additional constraints such that  $\frac{c_i}{c_j}$  being a rational function of  $C$ -minors for all non-vanishing  $c_i$  in the added row of  $C'$ , we call this soft limit a *rational soft limit*. When the soft limit of the auxiliary line is a rational soft limit, then the no-bridge diagram with the auxiliary momentum line can have a rational top-form if and only if the no-bridge diagram has a rational top-form.

We first consider the free parameters  $\alpha$ . The  $C$  matrix parameters  $\alpha_C$  that can be denoted by  $\mathbf{R}(M_C)$  is also  $\mathbf{R}(M_{C'})$ . The additional  $C'$  elements,  $c_i$ , are of the form  $c_r \mathbf{R}(\alpha_C)$  (indicating a rational soft limit for  $c_r \neq 0$ ). Since  $c_r$  is naturally  $\mathbf{R}(M_{C'})$ , all free parameters in  $C'$  are then rational functions of the minors, i.e., the top-form is rational. Conversely, given a linear auxiliary-bridge and a rational soft-limit, any  $C$  parameter denoted by  $\mathbf{R}(M_{C'})$  can be expanded in  $\mathbf{R}(M_C)$  directly, according to the procedure given above.

Thus let us study the geometric constraints. Geometric constraints are linear relations among columns of the constraint  $C$ -matrix. In fact the total space is taken to be a  $(k-1)$ -dimension projective space. Each column, indexed by the external line, can be mapped to a point in the projective space. For the diagrams which can be constructed by attaching BCFW-bridges, the constraints are co-planarity constraints imposed on



the points of external legs [19]. For those no-bridge diagrams, after attaching the auxiliary lines, the geometric constraints in  $C'$  are still co-planarity constraints. Hence we only need to be concerned with the evolution of the geometric constraints under a rational soft limit.

The simplest case corresponds to untangled geometric constraints in  $C'$ , with the co-planarity constraints in the form,

$$(i_1 i_2 \cdots i_m)^{m-1}.$$

If one of the indices, say,  $i_m$ , in above constraints denotes the auxiliary line, then the geometric constraint becomes  $(i_1 i_2 \cdots i_{m-1})^{m-2}$  under the soft-limit. If none of the indices denote the auxiliary line, then the geometry is invariant for  $m < k$ . As  $k \rightarrow k-1$  under the soft limit the geometric constraint for  $m = k$  vanishes upon taking the soft limit.

Given a generic set of untangled geometric constraints, momenta are constrained to be co-planar in the projective space under the soft limit. The geometric picture is, however, not so clear yet for the tangled constraints upon taking the soft limit: For example, what is the geometry resulted for  $((i_1 i_2 \cap i_3 i_4) i_5 \cdots i_m)$  after the soft limit is taken on  $i_1$ ? We will leave the geometric explanation in a future work. For the time being we will proceed with the algebraic route to arrive at the top form.

In general, the geometric constraints in  $C'$  can be expanded as

$$\begin{aligned} F'_1 &= \sum_{i=k+1}^n c_i F_1^{c_i}, & F'_2 &= \sum_{i=k+1}^n c_i F_1^{c_i}, \\ \cdots & & F'_{n-k-1} &= \sum_{i=k+1}^n c_i F_{n-k-1}^{c_i}, \\ \cdots & & F'_M &= \sum_{i=k+1}^n c_i F_M^{c_i}, \end{aligned} \tag{5.1}$$

where  $M$  being an integer. There are no higher order terms with respect to  $c_i$ . In fact if there are higher order terms, they can be factorized into linear polynomials, either with rational minors of  $C$  as coefficients or with non-rational minors. In the former case, one of the linear polynomials can be redefined as the geometry constraints. For the later case, some  $c_i/c_j$  are non-rational, a case which is beyond the scope of this paper.

Among the constraints in Eq. 5.1, we can choose arbitrary  $n - k - 1$  equations to solve for  $c_i/c_r$ . We can then substitute the solutions of  $c_i/c_r$  to obtain all the geometric constraints of  $C$  resulted from the soft-limit.

## 6 More Examples

### An $\overline{MHV}$ example

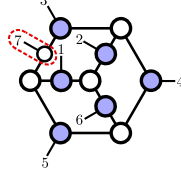


**Figure 3.** An  $\overline{MHV}$  example

In this subsection we give an example in a different situation—an auxiliary line connected to a white vertex—using an  $\overline{MHV}$  example (Fig. 3) for illustration. Attaching an auxiliary line enables the BCFW-reduction to identity by the following chain:  $(7, 3) \rightarrow (7, 5) \rightarrow (3, 4) \rightarrow (2, 3) \rightarrow (4, 5) \rightarrow (3, 4) \rightarrow (1, 3) \rightarrow (4, 6) \rightarrow (3, 7)$ . Before adding Bridge-(7, 5) the on-shell diagram is planar. The Grassmannian constraints (tabulated in the first row of Tab. 2) and the top-form can be obtained directly from the permutation [3]:

$$\frac{1}{(1234)(2345)(3456)(4567)(5671)(6712)(7123)}.$$

**Table 2.** Geometric constraints

	$(2(345)^2 6)^3$	$(345)^2$	$(5671)^3$	$(7123)^3$
$(7, 5)$	$(2346)^3$	$(3457)^3$	$(5671)^3$	$(7123)^3$
$(7, 3)$		$(3457)^3$	$(5671)^3$	$(7123)^3$

The transformation of constraints when adding the bridges  $(7, 5)$  and  $(7, 3)$  is shown in the second and third rows of Tab. 2; the top-form of  $\mathcal{A}_7^4$  becomes:

$$\frac{-(2467)^2}{(2347)(1246)(2456)(3457)(2346)(4567)(1567)(1267)(1237)}$$

Without loss of generality, we choose the first four columns of  $\hat{C}$  matrix to be identity:

$$\begin{pmatrix} \mathbf{e}_1 & \mathbf{e}_2 & \mathbf{e}_3 & \mathbf{e}_4 & & & \vec{c} \\ 1 & 0 & 0 & 0 & * & * & c_1 \\ 0 & 1 & 0 & 0 & * & * & c_2 \\ 0 & 0 & 1 & 0 & * & * & c_3 \\ 0 & 0 & 0 & 1 & * & * & c_4 \end{pmatrix}.$$

Then the last column can be represented by columns 1 to 4 as:

$$\vec{c} = c_1 \mathbf{e}_1 + c_2 \mathbf{e}_2 + c_3 \mathbf{e}_3 + c_4 \mathbf{e}_4.$$

In this way we can rewrite the minor involves the column-7 as:

$$\begin{aligned} (1237) &= c_4(1234) & (1567) &= c_2(1256) + c_3(1356) \\ (1267) &= c_3(1263) & (2467) &= c_1(2461) + c_3(2463) \\ (2347) &= c_1(1243) & (3457) &= -c_1(1345) - c_2(2345) \\ (4567) &= -c_1(1456) - c_2(2456) - c_3(3456) \end{aligned}$$

Let us study the three poles in  $\mathcal{A}_7^4$ . Since there is no constraint in  $\mathcal{A}_6^4$  we should integrate over all of these three poles and remove three coefficients. At last, there is only one coefficient left, and the rest can be re-expressed in the former:

$$c_4 \rightarrow 0, c_1 \rightarrow -\frac{(2345)}{(1345)}c_2, c_3 \rightarrow -\frac{(1256)}{(1356)}c_2.$$

The remaining coefficient in the top-form is

$$\frac{dc_2}{c_2},$$

which can be fixed by one of the columns in  $\hat{C}^\perp$  (noting that  $\hat{C}^\perp$  have one more column than  $C^\perp$ , which can be removed directly).

Finally, the top-form of  $\mathcal{A}_6^4$  becomes:

$$\frac{1 - [(2345)(1246)(1356) - (1256)(2346)(1345)]^2}{f_p (1246)(2456)(1345)(2346)(1356)(1235)},$$

where  $f_p = (1234)(2345)(3456)(4561)(5612)(6123)$ . This can also be simplified as

$$\begin{aligned} &- f_p(142356) - f_p(143265) + f_p(132456) \\ &- f_p(132654) + f_p(123465) - f_p(123465). \end{aligned}$$

### An NMHV example with no external BCFW-bridge:

In this subsection we present the detailed calculation of a NMHV example (Fig. 4(b)). An auxiliary external momentum line, marked leg-8, is added to the diagram before we can compute it by BCFW-reduction. The diagram transforms to a planar one by removing the bridges (2, 8), (6, 8) and (4, 2). The total decomposition chain is (2, 8)  $\rightarrow$  (6, 8)  $\rightarrow$  (4, 2)  $\rightarrow$  (1, 2)  $\rightarrow$  (2, 3)  $\rightarrow$  (2, 4)  $\rightarrow$  (4, 5)  $\rightarrow$  (4, 6)  $\rightarrow$  (6, 7)  $\rightarrow$  (1, 6)  $\rightarrow$  (6, 8). Before adding Bridge-(4, 2) the top-form of the planar sub-diagram is

$$\frac{1}{(1234)(2345)(3456)(4567)(5678)(6781)(7812)(8123)}$$

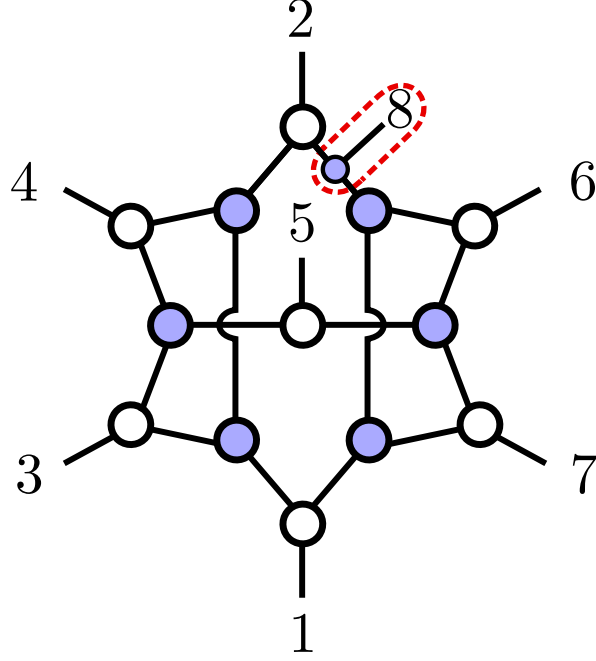


**Figure 4.** A nonplanar NMHV 4-loop leading singularity.

**Table 3.** The evolution of the geometric constraints in the NMHV example

	$(123)^2$	$(345)^2$	$(567)^2$	$(781)^2$
$(4, 2)$	$(1234)^3$	$(345)^2$	$(567)^2$	$(781)^2$
$(6, 8)$	$(1234)^3$	$(345)^2$	$(567)^2$	$(6781)^3$
$(2, 8)$	$(1234)^3$	$(345)^2$	$(567)^2$	

with constraints tabulated in the first row of Tab. 3.

After attaching all the BCFW-bridges we obtain the top-form integrand,

$$\frac{1}{(1234)(2345)(3456)(4567)(1567)(8672)(6781)} \\ \times \frac{(1347)(6721)^3}{(7812)(3167)(1237)(1247)(1286)}$$

with the geometric constraints tabulated in the last rows of Tab. 3. We can thus expand

the rank-4 minors into the rank-3 minors

$$\begin{aligned}
(1234) &= (123)c_4 & (2345) &= -(235)c_4 + (234)c_5 \\
(1237) &= (123)c_7 & (3167) &= -(317)c_6 + (316)c_7 \\
(1286) &= -(126) & (6721) &= -(721)c_6 + (621)c_7 \\
(8672) &= -(672) & (3456) &= (356)c_4 - (346)c_5 \\
(6781) &= -(671) & (1347) &= -(137)c_4 + (134)c_7 \\
(7812) &= (712) & (1247) &= -(127)c_4 + (124)c_7 \\
(1567) &= (167)c_5 - (157)c_6 + (156)c_7 \\
(4567) &= (467)c_5 - (457)c_6 + (456)c_7 .
\end{aligned}$$

Solving all the additional constraints incurred from the auxiliary line and the vertex we obtain:

$$c_4 \rightarrow 0, \quad c_5 \rightarrow 0, \quad c_7 \rightarrow \frac{(457)}{(456)}c_6,$$

with the final top-form integrand being

$$\frac{1}{f_p} \cdot \frac{(134)(357)[(457)(126) - (456)(127)]^3}{(124)(126)(135)(145)(267)(367)(457)^2},$$

and  $f_p = (123)(234)(345)(456)(567)(671)(712)$ . Applying the Plucker relations the integrand  $\frac{1}{f(C)}$  takes the form:

$$\begin{aligned}
& \frac{(125)}{(124)(126)(167)(235)(257)(143)(345)(567)} \\
& + \frac{(125)}{(124)(127)(165)(235)(267)(143)(345)(567)} \\
& + \frac{(125)}{(123)(126)(167)(234)(145)(257)(345)(567)} \\
& + \frac{(125)}{(123)(127)(165)(234)(145)(267)(345)(567)} . \tag{6.1}
\end{aligned}$$

It is, however, hard to use the Plucker relations to further simplify the above expression. A simpler technique is to parametrize the  $C$  matrix as

$$\begin{array}{ccccccc}
1 & 2 & 3 & 4 & 5 & 6 & 7 \\
\left( \begin{array}{ccccccc}
* & * & * & * & 0 & * & * \\
* & * & * & * & 0 & * & * \\
c_1 & c_2 & c_3 & 0 & 1 & 0 & c_7
\end{array} \right)
\end{array}$$

and expand the three-column minors in the two-column minors. Then the first term in (6.1) can be written as

$$\begin{aligned}
& \frac{-(12)(36)}{(124)(126)c_7(16)(23)(27)c_3(14)(34)(67)(36)} \\
&= \frac{-1}{(124)(126)(27)c_3(14)(34)(67)c_7(36)} \\
&+ \frac{1}{(124)(126)c_7(16)(37)c_3(24)(34)(67)} \\
&= \frac{-1}{(124)(126)(257)(134)(345)(567)(367)} \\
&- \frac{1}{(124)(126)(167)(234)(357)(345)(567)}. \tag{6.2}
\end{aligned}$$

Similarly we can rewrite the second term to fourth term in (6.1) as

$$\begin{aligned}
(II) &= \frac{1}{(124)(127)(167)(346)(235)(345)(567)} \\
&+ \frac{1}{(124)(127)(134)(267)(356)(345)(567)}; \tag{6.3}
\end{aligned}$$

$$\begin{aligned}
(III) &= \frac{1}{(123)(126)(143)(467)(275)(345)(567)} \\
&+ \frac{1}{(123)(126)(243)(467)(175)(345)(567)}; \tag{6.4}
\end{aligned}$$

$$\begin{aligned}
(IV) &= \frac{1}{(123)(127)(143)(267)(456)(345)(567)} \\
&+ \frac{1}{(123)(127)(234)(167)(456)(345)(567)}. \tag{6.5}
\end{aligned}$$

**A final example: an on-shell diagram with two auxiliary lines**

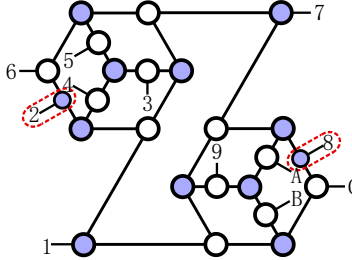


**Figure 5.** An  $N^4$ MHV example with two auxiliary lines

Our method can also tackle on-shell diagrams needing more than one auxiliary lines. Let us take, for example, the diagram,  $\mathcal{A}_{10}^4$ , in Fig. 5. After attaching the BCFW bridges recursively

$$\begin{aligned} (C8) &\rightarrow (A8) \rightarrow (62) \rightarrow (42) \rightarrow (34) \rightarrow (23) \rightarrow (12) \rightarrow (45) \\ &\rightarrow (34) \rightarrow (46) \rightarrow (37) \rightarrow (78) \rightarrow (27) \rightarrow (79) \rightarrow (7A) \\ &\rightarrow (AB) \rightarrow (2A) \rightarrow (AC), \end{aligned}$$

we obtain the integrand  $f(C')$  of the top-form:

$$\begin{aligned} &\frac{1}{(56789A)(6789AC)(5679AB)(789ABC)(89ABC1)(BC1246)} \\ &\times \frac{1}{(ABC134)(9ABC13)(BC1236)(BC1234)(C12346)(BC1345)} \\ &\times \frac{(5679AC)^3(BC1346)^3}{(123456)(234567)(5678AC)(45679A)(345679)(56789C)}. \end{aligned} \quad (6.6)$$

The geometric constraints are immediately obtained:

$$\begin{aligned} &(345)^2, (2456)^3, (5678AC)^3, (145679)^5 \\ &(9AB)^2, (8ABC)^3, (BC1246)^3, (7ABC13)^5. \end{aligned} \quad (6.7)$$

We first take the soft-limit on line-2. We use the gauge symmetry  $GL(k+2)/GL(k+1)$  to set the  $C''$  as

$$\begin{pmatrix} 1 & 2 & 3 & 4 & 5 & 6 & 7 & 8 & 9 & A & B & C \\ * & 0 & * & * & * & * & * & * & * & * & * & * \\ * & 0 & * & * & * & * & * & * & * & * & * & * \\ * & 0 & * & * & * & * & * & * & * & * & * & * \\ * & 0 & * & * & * & * & * & * & * & * & * & * \\ * & 0 & * & * & * & * & * & * & * & * & * & * \\ 0 & 1 & 0 & c_4 & c_5 & c_6 & c_7 & c_8 & c_9 & 0 & 0 & 0 \end{pmatrix}.$$

We arrive at five linearly independent equations with variables  $c_i$ ,  $i \in [4, 9]$  from the constraints  $(345)^2, (9AB)^2, (8ABC)^3, (7ABC13)^5, (5678AC)^3$  in Eq. 6.7

$$\begin{aligned} &(35x_1x_2x_3)c_4 - (34x_1x_2x_3)c_5 = 0 \\ &(BAx_1x_2x_3)c_9 = 0 \\ &(CABx_1x_2)c_8 = 0 \\ &(3ABC1)c_7 = 0 \\ &(C678A)c_5 + (5C78A)c_6 + (56C8A)c_7 + (567CA)c_8 = 0, \end{aligned} \quad (6.8)$$

where  $x_i$  denotes an arbitrary index of an external line in each of the constraint equations. Obviously the  $x$ 's are chosen in a way that the coefficients of  $c_i$  in above equations are made nonzero. We do not use the constraint containing line-2 in Eq. 6.7 since they do not give any constraints on the  $c_i$ . Performing the contour integration on  $dc_4 \cdots dc_9$  around the pole in above equations, the top-form becomes  $c_7 \rightarrow 0, c_8 \rightarrow 0, c_9 \rightarrow 0, c_4 \rightarrow \frac{(34x_1x_2x_3)}{(35x_1x_2x_3)}c_5, c_6 \rightarrow \frac{(678AC)}{(578AC)}c_5$ ; leaving one integration of  $dc_5$ . The poles in Eq. 6.6 are reduced as follows after integration,

$$\begin{aligned}
(5678AC) &= (578AC)(c_6 - \frac{(678AC)}{(578AC)}c_5) \\
(789ABC) &= -(89ABC)c_7 \\
(89ABC1) &= -(19ABC)c_8 \\
(9ABC13) &= -(13ABC)c_9 \\
(BC1345) &= -(135BC)(c_4 - \frac{(BC134)}{(BC135)}c_5)
\end{aligned} \tag{6.9}$$

Other minors are reduced accordingly by imposing the solutions of Eq. 6.8

$$\begin{aligned}
(123456) &= (13456), \quad (234567) = -(34567), \\
(BC1246) &= (146BC), \quad (BC1236) = (136BC), \\
(BC1234) &= (134BC), \quad (C12346) = -(1346C), \\
(345679) &= \frac{(34579)(678AC)}{(578AC)}c_5, \\
(56789C) &= \frac{(5678C)(789AC)}{(578AC)}c_5, \\
(56789A) &= \frac{(5678A)(789AC)}{(578AC)}c_5, \\
(6789AC) &= \frac{(789AC)(678AC)}{(578AC)}c_5, \\
(5679AB) &= \frac{(5679A)(79ABC)}{(579AC)}c_5, \\
(ABC134) &= \frac{(13ABC)(3479A)}{(3579A)}c_5, \\
(5679AC) &= -\frac{(567AC)(789AC)}{(578AC)}c_5, \\
(BC1346) &= -\frac{(134BC)(378AC)(5678C)}{(578AC)(3578C)}c_5, \\
(45679A) &= \frac{(4579A)(378AC)(5679A)}{(3579A)(578AC)}c_5.
\end{aligned}$$



Then we get the top-form of the on-shell diagram in Fig. 5 after taking the soft limit of line-2

$$\begin{aligned}
& \frac{1}{(13456)(1346C)(136BC)(13ABC)(146BC)(19ABC)} \\
& \times \frac{1}{(34567)(34579)(4578C)(5678A)(79ABC)(89ABC)} \\
& \times \frac{(134BC)(379AC)^2(5678C)^2(567AC)^3}{(579AC)(3578C)^2(5679A)^2(678AC)^2}.
\end{aligned} \tag{6.10}$$

The geometric constraints are

$$\begin{aligned}
& (3456)^2, (9AB)^2, (8ABC)^3, \\
& (BC146)^4, (15679)^4.
\end{aligned} \tag{6.11}$$

We take the soft-limit for line-8 and use the symmetry transformations of  $GL(k+1)/GL(k)$  to set the  $C'$  as

$$\begin{pmatrix}
1 & 3 & 4 & 5 & 6 & 7 & 8 & 9 & A & B & C \\
* & * & * & * & * & * & 0 & * & * & * & * \\
* & * & * & * & * & * & 0 & * & * & * & * \\
* & * & * & * & * & * & 0 & * & * & * & * \\
* & * & * & * & * & * & 0 & * & * & * & * \\
c_1 & c_3 & 0 & 0 & c_6 & 0 & 1 & 0 & c_A & c_B & c_C
\end{pmatrix},$$

where we have chosen  $c_4 = c_5 = c_7 = c_9 = 0$ . Using the constraints  $(345)^2, (456)^2, (9AB)^2, (BC146)^4, (15679)^4$  we can find the pole at  $c_3 \rightarrow 0, c_6 \rightarrow 0, c_1 \rightarrow 0, c_A \rightarrow \frac{(9Ax_1x_2)}{(9Bx_1x_2)}c_B, c_C \rightarrow \frac{(146C)}{(146B)}c_B$ , which are showed in the integrand as

$$\begin{aligned}
(13456) &= (3456)c_1, \\
(34567) &= -(3457)c_6, \\
(34579) &= (4579)c_3, \\
(136BC) &= (136B)(c_C - \frac{(136C)}{136B}c_B), \\
(79ABC) &= (79BC)(c_A + (\frac{(146C)(79AB)}{(146B)(79BC)} - \frac{(79AC)}{(79BC)})c_B).
\end{aligned}$$

Similar to the first soft-limit imposed on line-2, the other minors are reduced to

$$\begin{aligned}
(3578C) &= -(357C), (4578C) = -(457C), \\
(678AC) &= (67AC), (89ABC) = (9ABC), \\
(5678A) &= -(567A), (5678C) = -(567C), \\
\frac{(134BC)}{(146BC)} &= \frac{(134B)}{(146B)}, \\
(1346C) &= \frac{(1346)(146C)}{(146B)} c_B, \\
(5679A) &= \frac{(5679)(9A13)}{(9B13)} c_B, \\
(13ABC) &= -\frac{(1369)(13AB)(13BC)}{(139B)(136B)} c_B, \\
(19ABC) &= -\frac{(1469)(14BC)(19AB)}{(146B)(149B)} c_B, \\
(579AC) &= -\frac{(579A)(1469)(14BC)}{(149B)(146B)} c_B, \\
(379AC) &= -\frac{(379A)(1469)(46BC)}{(469B)(146B)} c_B, \\
(567AC) &= \left( \frac{(567A)(146C)}{(146B)} - \frac{(567C)(9A13)}{(9B13)} \right) c_B.
\end{aligned}$$

Thus we arrive at the integrand of the original on-shell diagram without auxiliary lines

$$\begin{aligned}
& \frac{1}{(1346)(1369)(3456)(3457)(4579)(5679)(579A)} \\
& \times \frac{(134B)}{(146C)(37AB)(13BC)(19AB)(79BC)(9ABC)} \\
& \times \frac{((367C)(379A)(146B) - (567A)(146C)(379B))^3}{(146B)^3(67AC)^2(357C)^2},
\end{aligned}$$

together with the geometry constraints  $(3456)^2, (9ABC)^2$ .

## 7 Summary and Outlook

We have obtained the top-form integrands for nonplanar leading singularities by BCFW-decompositions. In the cases that one cannot attach a BCFW-bridge we can add an auxiliary external momentum line judiciously so that the systematic method of BCFW-decompositions introduced by us in [18]. The original amplitude is recovered upon

taking the soft limit on the auxiliary momentum. This cocktail of strategies allows one to compute all leading singularity contributions from nonplanar diagrams of arbitrary higher-loops. We have also classified nonplanar on-shell diagrams according to whether they possess rational top-forms, and proved its equivalence to linear BCFW bridges (and correspondingly the rational soft limit for diagrams with no external BCFW-bridges). With the chain of BCFW-bridge decompositions obtained in this way, the rational top-forms of the nonplanar on-shell diagrams can be derived in a straightforward way. We stress that this method can be applied, in an obvious fashion, to the leading singularities of nonplanar multi-loop amplitudes beyond MHV.

An immediate question is whether all on-shell diagrams representing nonplanar leading singularities belong to this class, so that all leading singularities of nonplanar amplitudes can be expressed in rational top-forms.

Top-form, being simple and compact, is a great tool to uncover hidden symmetries (e.g. the Yangian symmetry beyond planarity [17]) which are otherwise highly tangled in nonplanar leading singularities. Combined with the method of generalized unitarity cuts, top-form holds promise in constructing the integrals as well as revealing the symmetries and dualities of nonplanar scattering amplitudes at loop-level.

Mathematically our method of performing the BCFW decompositions is related to the toric geometry arisen in the characterization of Matroid Stratification. Further investigation on the relationship between BCFW decompositions and Matroid Stratification will also shed light on the geometry of underlying Grassmannian manifolds.

## 8 Acknowledgments

G. Chen thanks Nima Arkani-Hamed for helpful discussion and useful comments. We thank Peizhi Du, Shuyi Li and Hanqing Liu for constructive discussion. Yuan Xin thanks Bo Feng for the enlightening lectures on the recent developments in scattering amplitude research. This research project has been supported by the Fundamental Research Funds for the Central Universities under contract 020414340080, the Youth Foundation of China under contract 11405084, the Jiangsu Ministry of Science and Technology under contract BK20131264. We also acknowledge 985 Grants from the Ministry of Education, and the Priority Academic Program Development for Jiangsu Higher Education Institutions (PAPD).

## References

- [1] A. Postnikov, ArXiv Mathematics e-prints (2006), [math/0609764](#).

- [2] S. Franco, D. Galloni, and A. Mariotti, *Journal of High Energy Physics* **2014**, 1 (2014).
- [3] N. Arkani-Hamed, J. L. Bourjaily, F. Cachazo, A. B. Goncharov, A. Postnikov, *et al.*, (2012), [arXiv:1212.5605 \[hep-th\]](#) .
- [4] N. Arkani-Hamed, F. Cachazo, C. Cheung, and J. Kaplan, *Journal of High Energy Physics* **3**, 110 (2010), [arXiv:0903.2110 \[hep-th\]](#) .
- [5] M. F. Paulos and B. U. W. Schwab, *JHEP* **1410**, 31 (2014), [arXiv:1406.7273 \[hep-th\]](#) .
- [6] Y. Bai and S. He, (2014), [arXiv:1408.2459 \[hep-th\]](#) .
- [7] T. Bargheer, Y. t. Huang, F. Loebbert and M. Yamazaki, “Integrable Amplitude Deformations for N=4 Super Yang-Mills and ABJM Theory,” *Phys. Rev. D* **91**, no. 2, 026004 (2015) [[arXiv:1407.4449 \[hep-th\]](#)].
- [8] L. Ferro, T. Lukowski, and M. Staudacher, (2014), [arXiv:1407.6736 \[hep-th\]](#) .
- [9] S. Franco, D. Galloni, A. Mariotti, and J. Trnka, (2014), [arXiv:1408.3410 \[hep-th\]](#) .
- [10] H. Elvang, Y.-t. Huang, C. Keeler, T. Lam, T. M. Olson, *et al.*, (2014), [arXiv:1410.0621 \[hep-th\]](#) .
- [11] N. Arkani-Hamed, J. Bourjaily, F. Cachazo, and J. Trnka, *Journal of High Energy Physics* **2012**, 1 (2012).
- [12] N. Beisert, J. Henn, T. McLoughlin, and J. Plefka, *Journal of High Energy Physics* **4**, 85 (2010), [arXiv:1002.1733 \[hep-th\]](#) .
- [13] J. Broedel, M. de Leeuw, and M. Rosso, *JHEP* **1406**, 170 (2014), [arXiv:1403.3670 \[hep-th\]](#) .
- [14] J. Broedel, M. de Leeuw, and M. Rosso, (2014), [arXiv:1406.4024 \[hep-th\]](#) .
- [15] N. Beisert, J. Broedel, and M. Rosso, *Journal of Physics A: Mathematical and Theoretical* **47**, 365402 (2014).
- [16] D. Chicherin, S. Derkachov, and R. Kirschner, *Nuclear Physics B* **881**, 467 (2014).
- [17] P. Du, G. Chen, and Y.-K. E. Cheung, *Journal of High Energy Physics* **2014**, 1 (2014) .
- [18] B. Chen, G. Chen, Y. K. E. Cheung, Y. Li, R. Xie and Y. Xin, “Nonplanar On-shell Diagrams and Leading Singularities of Scattering Amplitudes,” [arXiv:1411.3889 \[hep-th\]](#).
- [19] B. Chen, G. Chen, Y. K. E. Cheung, R. Xie and Y. Xin, “Top-forms of Leading Singularities in Nonplanar Multi-loop Amplitudes,” [arXiv:1506.02880 \[hep-th\]](#).
- [20] Z. Bern, E. Herrmann, S. Litsey, J. Stankowicz, and J. Trnka, (2014), [arXiv:1412.8584 \[hep-th\]](#) .

- [21] N. Arkani-Hamed, J. L. Bourjaily, F. Cachazo, A. Postnikov, and J. Trnka, (2014), [arXiv:1412.8475 \[hep-th\]](#) .
- [22] S. Franco, D. Galloni, B. Penante, and C. Wen, (2015), [arXiv:1502.02034 \[hep-th\]](#) .
- [23] M. Sogaard and Y. Zhang, JHEP **1412**, 006 (2014) doi:10.1007/JHEP12(2014)006 [arXiv:1406.5044 [hep-th]].
- [24] L. Bianchi and M. S. Bianchi, Phys. Rev. D **89**, no. 12, 125002 (2014) doi:10.1103/PhysRevD.89.125002 [arXiv:1311.6464 [hep-th]].
- [25] R. de Mello Koch, G. Kemp, B. A. E. Mohammed and S. Smith, JHEP **1210**, 144 (2012) doi:10.1007/JHEP10(2012)144 [arXiv:1206.0813 [hep-th]].
- [26] J. M. Henn, A. V. Smirnov and V. A. Smirnov, JHEP **1403**, 088 (2014) doi:10.1007/JHEP03(2014)088 [arXiv:1312.2588 [hep-th]].
- [27] F. Caola, J. M. Henn, K. Melnikov and V. A. Smirnov, JHEP **1409**, 043 (2014) doi:10.1007/JHEP09(2014)043 [arXiv:1404.5590 [hep-ph]].
- [28] S. J. Bidder, N. Bjerrum-Bohr, L. J. Dixon, and D. C. Dunbar, [Physics Letters B \*\*606\*\*, 189 \(2005\)](#).
- [29] A. Neitzke, Proceedings of the National Academy of Sciences **111**, 9717 (2014).
- [30] D. Xie and M. Yamazaki, Journal of High Energy Physics **2012**, 1 (2012).
- [31] N. Arkani-Hamed, J. L. Bourjaily, F. Cachazo, and J. Trnka, [Phys.Rev.Lett. \*\*113\*\*, 261603 \(2014\), arXiv:1410.0354 \[hep-th\]](#) .
- [32] H. Johansson, D. A. Kosower, K. J. Larsen, and M. Sogaard, (2015), [arXiv:1503.06711 \[hep-th\]](#) .
- [33] S. Franco, D. Galloni, B. Penante, and C. Wen, arXiv preprint arXiv:1502.02034 (2015).
- [34] Z. Bern, J. Carrasco, H. Johansson, and R. Roiban, [Phys.Rev.Lett. \*\*109\*\*, 241602 \(2012\), arXiv:1207.6666 \[hep-th\]](#) .
- [35] R. Frassek and D. Meidinger, arXiv:1603.00088 [hep-th].
- [36] Z. Bern, E. Herrmann, S. Litsey, J. Stankowicz and J. Trnka, arXiv:1512.08591 [hep-th].
- [37] E. Herrmann and J. Trnka, arXiv:1604.03479 [hep-th].
- [38] Z. Bern, L. J. Dixon, D. C. Dunbar and D. A. Kosower, “One loop n point gauge theory amplitudes, unitarity and collinear limits,” Nucl. Phys. B **425**, 217 (1994) [hep-ph/9403226].
- [39] M. Bullimore, “Inverse Soft Factors and Grassmannian Residues,” JHEP **1101**, 055 (2011) [arXiv:1008.3110 [hep-th]].

- [40] A. Volovich, C. Wen and M. Zlotnikov, “Double Soft Theorems in Gauge and String Theories,” arXiv:1504.05559 [hep-th].
- [41] P. Mastrolia, E. Mirabella, G. Ossola and T. Peraro, “Scattering Amplitudes from Multivariate Polynomial Division,” Phys. Lett. B **718**, 173 (2012) [arXiv:1205.7087 [hep-ph]].
- [42] P. Mastrolia and G. Ossola, “On the Integrand-Reduction Method for Two-Loop Scattering Amplitudes,” JHEP **1111**, 014 (2011) [arXiv:1107.6041 [hep-ph]].
- [43] B. Feng and R. Huang, Journal of High Energy Physics **2013**, 1 (2013).
- [44] Y. Zhang, Journal of High Energy Physics **2012**, 1 (2012).
- [45] Z. Bern, L. Dixon, D. C. Dunbar, and D. A. Kosower, Nuclear Physics B **425**, 217 (1994), [hep-ph/9403226](#) .
- [46] Z. Bern, L. Dixon, D. C. Dunbar, and D. A. Kosower, Nuclear Physics B **435**, 59 (1995).
- [47] Z. Bern, L. J. Dixon, and V. A. Smirnov, Physical Review D **72**, 085001 (2005).
- [48] F. Cachazo, arXiv preprint arXiv:0803.1988 (2008).
- [49] F. Cachazo, M. Spradlin, and A. Volovich, Physical Review D **78**, 105022 (2008).
- [50] R. Britto, F. Cachazo, and B. Feng, Phys. Rev. D **71**, 025012 (2005), [hep-th/0410179](#) .
- [51] R. Britto, F. Cachazo, and B. Feng, Nuclear Physics B **715**, 499 (2005), [hep-th/0412308](#) .
- [52] R. Britto, F. Cachazo, B. Feng, and E. Witten, Physical Review Letters **94**, 181602 (2005), [hep-th/0501052](#) .
- [53] B. Feng and M. Luo, Frontiers of Physics **7**, 533 (2012), [arXiv:1111.5759 \[hep-th\]](#) .
- [54] L. Ferro, T. Lukowski, C. Meneghelli, J. Plefka, and M. Staudacher, ArXiv e-prints (2013), [arXiv:1308.3494 \[hep-th\]](#) .
- [55] I. M. Gelfand, R. M. Goresky, R. D. MacPherson, and V. V. Serganova, Advances in Mathematics **63**, 301 (1987).
- [56] N. E. Mnëv, in *Topology and geometry - Rohlin seminar* (Springer, 1988) pp. 527–543.
- [57] R. Kleiss and H. Kuijf, Nuclear Physics B **312**, 616 (1989).